HIGH CHROME REFRACTORY CHARACTERIZATION: PART II. ACCUMULATION OF SPINEL CORROSION DEPOSITS IN RADIOACTIVE WASTE GLASS MELTERS

C. M. Jantzen,‡ K. J. Imrich,† K.G.Brown,* and J.B. Pickettƒ
Savannah River National Laboratory
Savannah River Nuclear Solutions
Aiken, SC 29808

Keywords: refractory, corrosion, melter life, melter accumulation

ABSTRACT

High Cr_2O_3 containing Monofrax™ K-3 is a robust refractory that is used in radioactive waste glass melters worldwide. Monofrax™ K-3 contains highly reduced phases. Conversely, many of the radioactive feeds being processed are highly oxidizing. The K-3 refractory corrosion rates in oxidizing (high nitrate) feeds were ~1.8-2.8 times higher than the rates determined using reducing feeds. The corrosion product formed is a mixture of spinel and glass (slag) that can accumulate on the melter floor. A methodology to calculate the depth of slag deposits from refractory corrosion is presented and verified with slag measurements from the Defense Waste Processing Facility (DWPF) melter after it had processed oxidized feeds for 1.75 years. The calculations show that had the facility continued to process oxidized feeds the melter lifetime, based on when the deposits could have reached and blocked the pour spout riser, would have been ~4.5 years. The DWPF changed to a reducing flowsheet after ~3 years of operation. The lifetimes of Melter #1 and Melter #2, assuming a failure due to pour spout blockage, are calculated as 7.7-12 years based on corrosion rates measured with reducing feeds. Lifetimes of 9 and >11 years have actually been achieved.

1.0 INTRODUCTION

Monofrax™ K-3 refractory has been used to line the High Level Waste (HLW) melters at the Savannah River Site (SRS), e.g. the Defense Waste Processing Facility (DWPF), and at West Valley Nuclear Services (WVNS). In addition, Monofrax™ K-3 was the refractory lining of Duratek's Duramelter 5000 at the SRS M-Area facility where high nitrate Low Level Mixed Waste (LLMW) waste was being vitrified. Monofrax™ K-3 has also been used in Hanford's HLW and Low Activity Waste (LAW) melter design. In addition, Monofrax™ K-3 is being used in HLW melters in Japan.

‡ carol.jantzen@srnl.doe.gov; Fellow and Distinguished Life Member American Ceramic Society
† ken.imrich@srnl.doe.gov
* current address Department of Civil and Environmental Engineering,Vanderbilt University, Nashville, TN 37235, kevin.g.brown@vanderbilt.edu
ƒ pickett.john@bellsouth.net, retired Savannah River Site, Fellow American Ceramic Society

Previous scale melter testing of the Monofrax™ K-3 refractory at the Savannah River National Laboratory (SRNL) had been performed using only reducing feeds containing minimal concentration of oxidizers (nitrate and nitrite). Currently, reduced feeds are being processed in the DWPF but in 1994 during DWPF non-radioactive startup the feeds were very oxidizing. [2] The feeds that were vitrified in the SRS M-Area facility and in the WVNS HLW melter were also highly oxidizing. Highly oxidizing HLW and LAW wastes will also be vitrified at Hanford at the Waste Treatment and Immboilization Plant (WTP).[1] The flowsheet is oxidizing due to (1) the high nitrate content of the feeds which gives off oxygen during denitration in the melter, and (2) the intent to bubble air into the melt to increase throughput. The characterization and corrosion data, the modeling of spinel accumulation from the refractory under various REDOX conditions, and validation of the depth of the spinel deposits from the non-radioactive startup testing in DWPF are, therefore, relevant to the startup of the WTP. The relative oxidizing nature of the wastes at the SRS, WVNS and WTP were described in Part I [2] of this study in terms of their nitrate and nitrite concentrations.

2.0 BACKGROUND

2.1 Operating Experience in Scaled Waste Glass Melters With Deposit Accumulation: Calcined and/or Reducing Feeds

Various pilot scale melters have been tested at the Savannah River National Laboratory (SRNL) and at Pacific Northwest National Laboratory (PNNL) with simulated SRS waste glass since ~1977 (Figure 1). During operation of liquid-fed and calcine-fed glass melters at PNNL and at SRS, large concentrations of insoluble crystalline phases were found to form when the melt exceeded the solubility of certain species or was too close to the liquidus temperature so that bulk crystallization of the melt pool occurred. All the melters were operated with a reducing flowsheet except the Integrated DWPF Melter System (IDMS). All pilot scale melters and DWPF Melter #1 were operated without agitation of any sort; i.e. no stirrers, no glass pumps [3], and no bubblers [4].

Crystalline phases, can form during melting of HLW or LAW glasses in those areas of the melt pool where the temperature drops below the liquidus temperature. [5,6,7,8,9,10,11,12] It should be noted that the measured activation energy for spinel crystallization in DWPF type waste glasses below the liquidus in an oxidizing melt pool is ~6 times more rapid than in a reducing melt pool, i.e. at $Fe^{+2}/\Sigma Fe \sim 0$ the activation energy for spinel formation is 17.7 kcal/mole while at $Fe^{+2}/\Sigma Fe \sim 0.5$ is only 2.9 kcal/mole. [13] Furthermore, melt pool insolubles such as RuO_2, Ag°, and Au° cause nucleation at the liquidus in ~2 hours while nucleation does not occur until ~48 hours when melt insolubles are absent. [14]

Crystalline deposits can also form as a reaction product of the corrosion of melter materials of construction. The driving force for refractory corrosion is discussed in Part I [2] and elsewhere [15]. Reviews of refractory corrosion in nuclear waste glass melters can be found in Reference 16.

Heterogeneous dissolution generally forms one or more new crystalline phases at the solid-liquid interface.[17] If the crystalline phase formed is not completely soluble in the glass or slag, it may form an impenetrable barrier so that, after its formation, further attack is prevented or slowed. [18] This is designated as a Type III "in situ" refractory by Lee et.al.[19] where the refractories and glass form a reaction layer that can be protective. Thus, an "in-situ" refractory surface is formed from the corrosion products provided that the products are not removed by melt stirring, bubbling, or other agitation. This type of "in-situ" refractory surface has been observed in pilot scale HLW melters lined with Monofrax™ K-3 where only natural melt convection was active. [20] However, during melt rotation or stirring, the saturated protective layer was removed from the refractory wall and replaced by fresh glass melt. [21] The fresh glass melt in contact with the refractory caused increased corrosion.

The insoluble spinels, whether derived from melt pool crystallization or Monofrax™ K-3 reaction product, settle to the floor of the melter and form viscous crystalline layers, often referred to as slag,[f] and the viscous material can adhere to the melter walls in a melter without agitation as noted above. Formation of crystalline material is undesirable because the partially crystallized melts are more viscous [22] which can cause difficulty in melting and discharging the glass. Melts free of crystalline material are Newtonian and obey the Vogel-Fulcher-Tammann (VFT) relationship at temperatures above the glass transition temperature. Melts containing ≤10 vol% crystals were found not to agglomerate in short 3 hour crucible melting tests. Agglomerates were defined as 10X larger than a single spinel crystal. Non-agglomerating spinel containing melts are Newtonian but obey the Einstein-Smoluchowsky equation for the diffusion of spherical particles through a liquid instead of VTF relation.[22] If melts with ≤10 vol% crystals agglomerate [23,24] they will become non-Newtonian. In the short 3 hour crucible tests, melts with ≥13 vol% crystals were all determined to be non-Newtonian due to the presence of agglomerates.[22] Once formed, crystalline species such as spinel are stable to temperatures of >1600°C [25], which is much greater than the typical 1150°C melt temperature in a Joule-heated melter. Thus spinel deposits, once formed, would be impossible to dissolve. Any melts in which the spinels agglomerate will be non-Newtonian and should be avoided.

Because both the Monofrax™ K-3 corrosion products [2,26] and the DWPF primary liquidus phase [11,12] are $Ni(Cr,Fe)_2O_4$ it is difficult to assess whether or not the nickel chrome ferrite crystalline species that accumulate on melter bottoms were formed by temperature excursions or by interaction with the Monofrax™ K-3 refractory unless a post melt analysis is performed. The only evidence regarding the differences in the composition of the spinels was obtained when an SRNL mini-melter failed and the glass at the Monofrax™ K-3 interface sidewall was sampled. The reaction product from the Monofrax™ K-3 was $Ni(Cr_{0.8}Fe_{0.2})_2O_4$ which is a Cr_2O_3 enriched spinel with considerable more Cr than the nominal

[f] Slag is generally considered a partially vitreous by-product of the process of smelting. When ores are smelted the slag produced is usually a mixture of metal oxides and silicon dioxide. Throughout this document, slag is defined as a mixture of transition metal spinels which may come from crystallization of the melt or spalling of refractory corrosion products, glass, and other crystalline silicate reaction products.

$Ni_{0.85}Mn_{0.15}(Fe_{0.8}Cr_{0.2})_2O_4$ spinel reported to crystallize from DWPF type glasses at the liquidus temperature [11].

Crystal formation in waste glass melters [27,28,29,30,31] was first observed in PNNL's Liquid-Fed Ceramic Melter (LFCM) in 1977 when defense waste glass formulations were being melted [27;28]. In 1979 PNNL observed crystal formation in the melt when commercial HLW glass formulations were melted in the Calcine-Fed Ceramic Melter (CFCM).[ξ] Subsequently, additional crystal formation was observed when defense waste glass formulations were melted in the CFCM. The dominant insoluble species found to have crystallized from defense waste glass was nickel iron spinel [30]. The spinel layer on the melter floor of the CFCM was ~12.7 cm thick and it was unclear as to whether the deposits formed from reaction with the Monofrax™ K-3 refractory or by crystallization of the melt pool since the composition of the spinel was not analyzed.

At the SRNL, a spinel layer of ~22.86 cm thick was formed during the Project 1941 large scale melter tests with calcine feeds in 1978 [29]. When the 1941 large scale melter was shut down after pouring 74 tons of waste glass over a 398 day period, it was dismantled to evaluate its service life.[32] Additional crystalline deposits up to approximately 2.54 cm thick and containing ~30 volume percent spinel were found on the walls of the Project 1941 pilot scale melter (2/5 DWPF scale) during testing at SRNL with reducing feeds The formation of this layer was attributed to reaction of the refractory with the glass although the spinel was not analyzed. This layer was viscous and appeared to remain on the wall of the melter refractory protecting it from further corrosion. Decreased melt viscosity (which caused increased melt convection) was found to remove the protective layer. The reaction zone was studied and considered typical of zones found on Monofrax™ K-3 in the commercial glass industry and in waste glass melters at the PNNL. [33,34].

Calcine feeding was found to accelerate crystal accumulation in waste glass melters, and was abandoned in favor of wet slurry feeding which simultaneously controls dusting of calcine feeds which were radioactive and hazardous constituent inhalation hazards. The deposition of melter bottom deposits in melters where the liquidus was controlled so that melt pool crystallization could not occur, are primarily from Monofrax™ K-3 refractory corrosion.[36] The existing data for slurry fed melters are summarized in Table 1 and in Reference 35. The lack of slag formation in the large scale melters summarized in Table 1 was attributed to better melter design, slurry feeding rather than pre-calcining, control of rheology and REDOX by formic acid addition, and more solubilizing frit compositions.[36]

Table 2 shows the relative corrosion rates observed in the various pilot scale melters tested at SRNL. The LSFM large scale melter had an average corrosion rate of ~1 mil/day during its two years of continuous operation. The LSFM processed only reduced DWPF formic acid flowsheet feeds which produced reduced glasses with SRNL 131 glass and SRNL165 glass with an average waste composition.[37] Spalling of the Monofrax™ K-3 was observed in the

[ξ] During the early studies of nuclear waste glass vitrification, the waste sludges were calcined into oxide powders. Currently the waste sludges are slurry fed also known as liquid fed.

LSFM, and the most aggressive corrosion was observed at the melt line and near the throat of the riser [38].

At the time the LSFM Monofrax™ K-3 refractory corrosion was being evaluated, the Carborundum Company identified the Monofrax™ K-3 corrosion mechanism as being a strong function of the nickel oxide and iron oxide in the glass where Ni and Fe in the glass exchange for Mg and Al in the refractory forming Cr-Ni-Fe spinel as a reaction product.[2, 38] Micrographs of the K-3 refractory taken from the LSFM after 2 years of operation clearly showed a Ni-Fe rich reaction layer [38].

In the Integrated DWPF Melter System (IDMS), about 30.5 cm of deposits remained after draining, which was a combination of melter bottom deposits and unmelted cold cap material. Maximum wear of the Monofrax™ K-3 refractory in the IDMS melter was observed at the bottom of the melter in the drain region. Approximately 5 cm of refractory was missing in this region [39]. Over the 7 years of operation of the IDMS, this amount of corrosion corresponded to approximately 0.78 mils/day (Table 2) similar to that measured during post mortem testing of the Large Scale Slurry Fed Melter (LSFM). It should be noted that the crystalline material from the bottoms of scale glass melters has also been found to accumulate at the base of pour spout risers where velocities can change during pouring events [38].

During the post melt evaluation of the IDMS melter, a sodium magnesium chromium silicate (krinovite, $NaMg_2CrSi_3O_{10}$) and a Cr-rich spinel were found by Jantzen and Lambert [39] in all of the glassy slag deposits removed from the floor of the IDMS melter during core drilling. Since the decomposition of chrome refractories used in the steel industry in the presence of SiO_2 [40] forms the following decomposition products: $MgO•SiO_2$ (protoenstatite), $2MgO•SiO_2$ (fosterite) and $MgO•Cr_2O_3$ (picrochromite), it was hypothesized [26] that the Mg containing krinovite represented one of the decomposition products of the K-3 refractory degradation after the MgO silicates (protoenstatite and fosterite) had further reacted with the Na_2O component of the simulated HLW glass being processed [39]. This mechanism is discussed in more detail in Part I.[2]

Additional Monofrax™ K-3 corrosion studies were recently conducted at the PNNL [41]. Waste glasses with Fe_2O_3 concentrations varying from 12.6 to 15.5 wt% were tested in the presence of an oxidizer (HNO_3) and a reductant (glycol as a substitute for formic acid/formate salt reductants). Accelerated K-3 corrosion was observed in the highly oxidized feeds. Elevated concentrations of Al_2O_3, Cr_2O_3, MgO, and MoO_3 were observed in the bottom drain and melt surface samples. The concentrations of these constituents increased with increased processing time.

Table 1 and Figure 1 provide a summary of the scaled glass melters, the DWPF melter (non-radioactive and radioactive), the respective melt pool surface areas, the years of continuous operation, the depth of any bottom deposits observed on melter evaluation post melt or during probing. The amount of glass that each melter processed in tons, and whether or not

the melter ran reducing (formic acid or a mixture of formic/nitric acids) or oxidizing flowsheets (nitric acid only) is also given in Table 1.

2.2 Operating Experience in DWPF Melter #1 With Deposit Accumulation: Oxidizing Feeds

After 1.75 years of DWPF operation with simulated oxidized feeds the melter was rodded to probe for crystalline deposits on the floor of the melter. An accumulation of ~6.35 cm (~2.5 inch) of deposits was noted and analyses performed indicated that the crystalline material was Cr_2O_3 enriched crystalline spinels. This concentration was considered atypical of the amount of spinel accumulated in other slurry fed large scale DWPF pilot scale melters. The comparison of the accumulation rates given in Table 1 demonstrates that the DWPF bottom deposit accumulation rate (centimeters/year) is more rapid than previously experienced in large pilot scale testing with slurry feeding and reducing flow sheets. Since the DWPF was operating an oxidizing flowsheet for initial operations compared to the reduced flowsheets tested at the pilot scale, the following studies were performed:

1-8. see Part I [2]
9. analyze the composition and phase identification of the DWPF bottom deposits
10. calculate spinel accumulation rates on the floor of the DWPF melter for oxidizing and reducing flowsheets from measured corrosion rates in crucible studies and pilot scale melters
11. verify the calculational method with the depth of the deposits rodded after 1.75 years of DWPF operation.

Part I [2] of this study addressed the results from items 1-8 while Part II addresses items 9-11 including summarizing all the melter accumulation deposits observed in pilot scale melters at SRS including the 1.75 years of non-radioactive processing in the full scale DWPF. While the data discussed in this manuscript were collected during DWPF startup, and DWPF has been operational for ~20 years, the data have never before been published.

3.0 EXPERIMENTAL

In March and April 1996 during non-radioactive DWPF testing (Proficiency Campaign 2 or PRO-2), deposits formed in the DWPF pour spout on several occasions. On March 30, 1996, glass samples and melter bottom deposits were obtained by inserting long rods with sample cups welded to the bottom of the rod through a nozzle in the melter dome until the bottom of the cup impacted a semi-solid "mushy" layer of deposits on the melter floor near the riser [42]. The melter was "rodded" to see if crystalline deposits had built up on the melter floor– particularly in the vicinity of the base of the DWPF riser. The concern was that accumulated crystalline material on the floor of the DWPF melter could be a source of the pour spout deposits and hence a potential causative agent of the pouring anomalies. Such a buildup at the base of the melter riser had been observed during the LSFM post mortem.[38]

The rodding of the melter showed two distinct layers of material. The bottom most layer, which was about 3.8 cm in depth, was of high density while the "mushy" layer was less dense and was about 2.54 cm in depth [42]. The total depth of the layer accumulated in

~1.75 years from DWPF initial startup was ~6.35 cm. No deposit accumulation or blockage was detected on the bottom of the melter near the riser [42].

The glass inside the two cups and the partially crystallized melter bottom deposits adhering to the underneath and bottom surfaces of the cups were characterized by SRNL at the request of DWPF Engineering. Visually, a layer of crystalline deposits adhered to the bottom of the cups and partially up the outside of the sample cups. The cups are ~10.16 cm high and impacted the bottom deposits vertically so that no crystalline deposits were found inside the cups or further up the rods above the cups.

The glass in the cups and the adherent melter bottom deposits on the bottom of the cups were analyzed at the Savannah River National Laboratory (SRNL) using the following techniques:

- Dissolution by Na_2O_2 fusion with an HCl uptake
  - ICP for Al, B, Ba, Ca, Cr, Cu, Fe, Li, Mg, Mn, Ni, P, Pb, Si, Sr, Ti, Zn
- Dissolution by HCl/HF microwave
  - ICP for Na, Zr
  - AA for K

where ICP-ES is Inductively Coupled Plasma Emission Spectroscopy and AA is Atomic Absorption Spectroscopy analysis. The deposits were also analyzed by X-ray Diffraction (XRD) to determine what the crystalline phases were. If the samples contained spinel crystals, qualitative phase identification was made. For certain samples, the quantitative amount of spinel present was also determined by XRD.

4.0 RESULTS

4.1 Chemical and Phase Analysis of DWPF Melter #1 Bottom Deposits

The chemical analyses indicated that the crystallized material adhering to the bottom of the sample cups was enriched in NiO, Fe_2O_3 and Cr_2O_3 compared to the glass within the sample cups (Table 3). The analyses of the non-crystallized glasses in Table 3 sum to 100±5 wt% while the analyses for all of the crystallized melter bottom deposits do not. This is because the highly crystallized deposits were very refractory and difficult to dissolve completely.

X-ray diffraction analysis confirmed that the crystallized melter bottom deposits adhering to the bottom of the sampler cup were Ni-Fe-Cr spinels. The melter bottom deposits contained between 25-34 wt% spinel and some RuO_2 compared to the glass adhering to the side of the rod which contained only 0.7-5.2 wt% spinel (Table 4). These DWPF melter bottom deposits (the denser and less dense layers) were similar in composition to the melter bottom deposits analyzed from the IDMS in that they were enriched in NiO, Fe_2O_3 and Cr_2O_3 [39].

4.2 Differences in Corrosion Rate Measurements

The “average loss of material” data shown in Table 2 provides a comparison of the measured corrosion rates in oxidized vs. reduced feeds and in oxidized feeds vs. pre-reacted glass. Table 2 also provides a comparison between pilot scale melter testing and crucible testing.

The "average loss of material" for oxidizing feeds, whether in a crucible or the 1/100th scale DWPF minimelter, was 1.40-1.57 mils/day versus measurements of 0.64-0.79 mils/day in SRNL165 glass or SRNL131 glass. Therefore, the ratio of the corrosion rates in oxidized feeds divided by the pre-reacted glass gives a range of ~1.8-2.5 times more corrosion in oxidizing feeds. Likewise, the comparison of oxidizing feed pilot scale melter corrosion rates (1/100th scale DWPF mini-melter average rate of 1.40 mils/day) to reducing feed pilot scale melter corrosion rates (LSFM and IDMS of 0.5 to 0.78 mils/day) in Table 2 suggests that oxidized feeds are ~1.8-2.8 times more aggressive to K-3 than reducing feeds.

The last comparison made from the data in Table 2 is that between pre-reacted glass and pilot scale melter rates with reducing feeds. The corrosion rates in pre-reacted glass (SRNL165 and SRNL131 glass) are 0.64-0.79 mils/day while the reducing feeds from pilot scale melters (LSFM and IDMS) are in the range of 0.5-0.78 mils/day while. The ratio of pre-reacted glass corrosion rates to the reducing melter feeds are in the range of 0.8-1.58 times. These data suggest that the use of pre-reacted glass is more representative of pilot scale melters operating with reducing flowsheets than pilot scale melters operating with oxidizing flowsheets.

4.3 Calculated Accumulation Rates of Monofrax™ K-3 Refractory Corrosion Deposits in the DWPF Melter

At the time that the DWPF melter was "rodded" on March 30, 1996, about ~6.35 cm of deposits had accumulated on the melter floor [42]. At this time the melter had been in operation for 1.75 years and had processed 2.79 x 10^5 pounds of glass during non-radioactive startup (between Facility Acceptance test FA-13 and Proficiency Campaign 2 or PRO-2). The corrosion rates measured in Part I [2] of this study provided linear corrosion rates for Monofrax™ K-3 in oxidized DWPF nitric acid feeds. Based on the "average loss of material" given in Equation 2 of Part I – a calculation can be performed (Appendix A) to estimate the amount of corrosion products that would be available after the 1.75-year operational life of the DWPF melter with oxidized feed, i.e. at the time the melter bottom was probed.

Probing of the DWPF melter after 1.75 years indicated ~6.35 cm of deposits had accumulated (a dense and less dense layer). The calculated accumulation based solely on the Monofrax™ K-3 corrosion rates measured in Part I of this study was 6.55 cm of slag (Table 1 and Table 2).

Similar calculations, performed for the different measured corrosion rates given in Part I for various pilot sale melters with reducing feeds and crucible studies with pre-reacted glass (ASTM C621), were also performed. In addition, accumulation amounts based on the DWPF design corrosion rates were also calculated for comparison (Table 2) assuming the same 1.75 year duration.

- Design rates (sidewall + lid + bottom) projected an accumulation of 14.6 cm of slag
- Design rates (melt line) projected an accumulation of 36.58 cm of slag

- Design rates (below melt line) projected an accumulation of 26.37 cm of slag
- Crucible tests in pre-reacted glass (1.75 years) projected an accumulation of 3.12-3.61 cm of slag

Clearly, the DWPF design basis for the sidewall + lid + bottom of the melter over predicted the potential amount of accumulation in 1.75 years by a factor of >2 and the crucible tests in pre-reacted glass under predicted the amount of slag accumulation by ~50%. Using the measured corrosion rates from the various SRNL pilot scale melters during testing with reduced feeds, the following accumulations can be predicted:

- LSFM operation (2 years) would have accumulated 2.79 cm of slag deposits
- IDMS operation near drain (7 years) = 15.22 cm of slag deposits

The depths calculated for the LSFM are approximately two times higher than those observed during melter analysis after draining but some deposits could have been lost during bottom draining. In the case of the IDMS the draining was a power drain and the depth of any deposits was indeterminate. These calculated depths are still minimal compared to the DWPF design rates since the LSFM and IDMS processed simulated waste glass with a reducing flowsheet.

It should also be noted that the formation of insoluble spinels in radioactive waste glass melters as a function of oxidation or reduction in the melt pool, the formation of an "in situ" refractory layer of these spinels on the refractory, and their accumulation in or near the pour spout is not unique. Spinels of the $MgAl_2O_4$ type occur when molten Al° and Mg° are oxidized to Al_2O_3 and MgO in the DIMOX™ process during Al° smelting.[43,44]

5.0 DISCUSSION

5.1 Accumulation Rates of Monofrax™ K-3 Refractory Corrosion in Oxidizing Vs. Reducing Feeds

The calculations given in Appendix A for the melters that were slurry fed compare the corrosion rates of the DWPF melter over its 1.75 years of operation based on the corrosion rates from Part I [2] of this study to (1) the corrosion rates measured in pilot scale melters such as the LSFM and IDMS with reducing feeds, (2) the DWPF design basis corrosion rates, and (3) the corrosion rates from crucible testing with SRNL131 and SRNL165 glass. Using the measured corrosion rates in Part I [2] and assuming a 35% spinel/65% glass mixture in the slag deposits that can accumulate on the bottom of a melter about 6.55 cm of deposits could have formed over the 1.75 years of operation with these oxidized feeds (Table 2). This accumulation compares very favorably with the probed deposit depth of ~6.35 cm, certainly given the likely errors associated with the depth measurement.

Note that the Cr_2O_3 in the glass is not used in the calculations of spinel accumulation from K-3 refractory corrosion; the amount of Cr_2O_3 available from the K-3 refractory based on the "average loss of material" is used instead. This use avoids complications with Cr_2O_3 variability in different feeds or in contamination during glass analyses from using steel

grinders. The calculations assume that the 0% liquidus temperature has not been violated, i.e. there has been no spinel precipitation from the melt pool. Thus the amount of spinel that can still accumulate due to K-3 refractory corrosion in oxidizing feeds is calculated and shown to limit melter life time, even when (1) the liquidus temperature has not been violated and (2) the melt pool is not agitated. Agitation will only increase the rate of K-3 corrosion since the brick is more reducing with depth away from the "hot wall" face.

The values given in Table 2 also verify the low corrosion rates measured for other SRS large scale melters, e.g. the LSFM and IDMS, with reducing feeds. In addition, the calculations demonstrate that the actual corrosion observed during the first 1.75 years of DWPF operation was one-third the design basis for the refractory walls below the melt line, which correspond to >26.4 cm of slag in 1.75 years at the design basis (Table 2).

The calculations indicate that at a corrosion rate of 0.5 mil/year experienced with the LSFM and reducing feeds it would take ~12 years for the spinel bottom deposits from K-3 (assuming no spinel accumulation from the melt pool) to reach the bottom height of the riser. At the sidewall the riser height is 16.5 cm but since the melter floor is indented in the center this corresponds to a height of 25.15 cm in the center of the melter. For the IDMS with a corrosion rate of 0.78 mils/day it would take ~ 7.5 years to begin to block the riser at the sidewall with deposits. Using the corrosion rates from the average mini-melter testing (melt and vapor) from Table 2 in oxidizing feeds (1.57 mils/day) suggest melter lifetimes of only 4.5 years to begin to block the riser in a non-agitated melt pool.

The accumulation depths given here are conservative for the following reasons:

- corrosion of the refractory will be greater with mechanical melt pool agitation vs. natural convection [21]
- corrosion of the refractory will be ~1.8-2.8 times greater with oxidizing feeds rather than reducing feeds [2]
- corrosion of the refractory will be ~1.3 times greater with higher Na_2O containing melts. [45]

5.2 Potential Impact of Monofrax™ K-3 Refractory Corrosion Products on Glass Durability

If the glass being discharged from the melter into the HLW canister contains spinels from the Monofrax™ K-3 refractory corrosion, no impact is anticipated on the glass durability. This conclusion is based on several factors. The spinels that form in the melt pool, from melt pool temperature excursions below the liquidus, are compositionally very similar to those spinels that form from the Monofrax™ K-3 refractory corrosion. For spinels that form from the melt the compositions have been measured [11,12] measured by microprobe analyses to be $(Ni_{0.85}Mn_{0.15})(Fe_{0.80}Cr_{0.20})_2O_4$, $(Ni_{0.95}Mn_{0.05})(Fe_{0.92}Cr_{0.08})_2O_4$, $(Ni_{0.77}Mn_{0.31}Mg_{0.02})(Fe_{0.95}Cr_{0.015}Al_{0.003}Ti_{0.002})_2O_4$ and contain no radionuclides.[ξ] The spinel that forms from the corrosion of the Monofrax™ K-3 refractory was reported in this study to compositionally be $Ni(Cr_{0.8}\,Fe_{0.2})_2O_4$ and also do not contain any radionuclides.[ξ]

[ξ] The only radionuclides that could be sequestered by these spinels are Ni^{59} and Ni^{63} and Fe^{55}. However, the Ni radioisotopes are 3 orders of magnitude lower than non-radioactive Ni and Fe^{55}, which has a relatively short

The spinels in the melt pool have been found to form on RuO_2 insolubles [9] in the melt but this is not observed for the spinels that form from the Monofrax™ K-3 refractory corrosion.[2] The presence of spinels from either the melt pool crystallization or from the Monofrax™ K-3 refractory corrosion will not impact the overall durability of the glass as shown by Jantzen and Bickford [8] as the glass is isotropic and the spinel is isotropic.

6.0 CONCLUSIONS

The K-3 corrosion was determined to be incongruent or heterogeneous in Part I [2]. As determined by previous researchers, the Monofrax™ K-3 refractory surface becomes depleted in Al_2O_3, MgO, and Cr_2O_3 leaving a porous outer corrosion layer that allows reaction with Fe_2O_3 and NiO from the waste glass. Glasses with higher Na_2O content appear to solubilize the Al_2O_3 component of the Monofrax™ K-3 more rapidly. Although the Monofrax™ K-3 brick does not contain NiO, its prime corrosion reaction product is $Ni(Cr,Fe)_2O_4$ spinel. Free energy and REDOX potential calculations in Part I [2] demonstrated that the DWPF high nitrate oxidizing feed and melt conditions likely act as driving forces for attack by oxidative dissolution of the highly reduced Monofrax™ K-3, i.e. the Monofrax™ K-3 is unstable in highly oxidized feeds based upon these computations.

The specific conclusions based on the studies and calculations performed indicate that oxidizing melter flowsheets can contribute or cause the following:

- increased accumulations of spinel deposits on the melter floor from the refractory corrosion relative to pilot scale melting with reducing flowsheet feeds
  - Decreased melter life in a non-agitated melt pool, i.e. 4.5 years compared to 7-12 years while spinels are not being formed at the liquidus temperature
  - Additional refactory corrosion will ensue if the melt pool is agitated as the K-3 brick becomes more reduced as the brick is corroded
  - An even shorter melter life will occur if 1-2% spinel is allowed to form in the glass by melter operation below the 0% liquidus temperature as this will create additional spinel slag (if spinels agglomerate and melts become non-Newtonian the 1-2% spinel will not be swept out of the melter during a pour)
- accelerated Monofrax™ K-3 refractory degradation relative to testing in pre-reacted glass by ASTM C621

These results indicate that the use of pre-reacted glass is more representative of pilot scale melters operating with reducing flowsheets and not representative of pilot scale melters

---

half-life, has decayed away since the waste was generated over 50 years ago. The non-radioacitve Ni in the waste is derived from the dissolution of Ni cladding from fuel rods and the non-radioactive Fe in the waste is derived from the use of ferrous sulfamate in the Purex process. The non-radioactive isotope concentrations are far in excess of the radioactive isotopes in the waste.

operating with oxidizing flowsheets. A modified crucible tests such as the one presented in Part I [2] should be used to determine corrosion rates in oxidized feeds.

7.0 ACKNOWLEDGMENTS

Many thanks are due to Alex Cozzi and Bruce Hardy of SRNL for their many helpful discussions about mechanisms by which melt pool deposits can form and be transported. The authors would like to gratefully acknowledge the assistance of SRNL's Analytic Development personnel. This paper was prepared in connection with work done under Contract Nos. DE-AC09-76SR00001, DE-AC09-96SR18500, DE-AC09-08SR22470 with the U.S. Department of Energy.

8.0 APPENDIX A

Step #	Calculation
1	Equation 2 (R^2=0.97) from Part I [2] Corrosion (mils)$_{K\text{-}3\ loss\ of\ material}$ = 1.225 + 1.34(638.75 days) = 857.15 mils in 1.75 years (638.75 days).
2	Convert depth (Step #1) from mils to cm: $(857.15\ mils)\left(\frac{inch}{1000\ mils}\right)(2.54\ cm/inch) = 2.18\ cm\ corroded\ in\ 1.75\ years$
3	K-3 surface area of the interior of the DWPF melter exposed to glass and/or vapor from the melt pool is approximately 6.317 m^2 (63174.07 cm^2)
4	Multiply the surface area (Step #3) by the depth of attack times the K-3 density: =(63174.07 cm^2)(2.18 cm)(3.9g/cc) = 5.37 x 10^5 g K-3 available to form bottom deposits after 1.75 years.
5	Multiply the grams of K-3 corroded (Step #4) by the amount of Cr_2O_3 (27 wt% fromTable 2 in Part I) in K-3 = (5.37 x 10^5 g K-3)(0.271 g Cr_2O_3/g K-3) = 1.46 x 10^5 g Cr_2O_3 or 956 moles Cr_2O_3 available to form melter bottom deposits
6	Since the spinel from the failed mini-melter provided an approximate composition for the Cr-rich spinel attached to the K-3 refractory during the melter autopsy (Section 2.1), the approximate composition used for slag (glass plus spinel) is $Ni(Cr_{0.8}Fe_{0.2})_2O_4$. This spinel contains 0.4 moles of Cr_2O_3. Therefore, dividing the 956 moles of Cr_2O_3 available (Step #5) by 0.4 moles of Cr_2O_3 necessary to make this spinel and then multiplying by the molecular weight of the $Ni(Cr_{0.8}Fe_{0.2})_2O_4$ spinel, gives the inventory of $Ni(Cr_{0.8}Fe_{0.2})_2O_4$ spinel that might be expected in the melter bottom deposits: $Ni(Cr_{0.8}Fe_{0.2})_2O_4$ gm = $\left(\frac{956\ moles Cr_2O_3}{0.4\ moles Cr_2O_3 / mole\ Ni(Cr_{0.8}Fe_{0.2})_2O_4}\right) * 228\ gms/mole$ = 5.45 x 10^5 g $Ni(Cr_{0.8}Fe_{0.2})_2O_4$
7	If the deposits were 100% spinel the volume of $Ni(Cr_{0.8}Fe_{0.2})_2O_4$ spinel in cc (cm^3) can be calculated by dividing by the density of a Ni-Fe-Cr spinel which is ~5.227-5.229 g/cc (PDF 23-1119) $Ni(Cr_{0.8}Fe_{0.2})_2O_4$ (cc) = $\frac{5.45 \times 10^5 \text{ grams } Ni(Cr_{0.8}Fe_{0.2})_2O_4}{5.229 \text{ g/cc}}$ = 1.04 x 10^5 cc spinel
8	Since the melter bottom deposits are a mixture of spinel and glass, an additional calculation must be performed. DWPF waste glass at 1150°C has a density of 2.105 g/cc [46]. The melter bottom deposits analyzed in this study are a mixture of 25-34 wt% spinel (Section 4.1). The deposits found on the walls of the Project 1941 melter were estimated to contain ~30 volume% (~45 wt%) spinel after cooling to room temperature while the DWPF bottom deposits had 25-34 wt% spinel when analyzed. Using an average of ~35 wt% spinel (middle of the observed range from 25-45 wt% spinel) and 65 wt% glass, the weighted density of the spinel/glass bottom deposits Spinel + glass (cc) = $\frac{5.45 \times 10^5 \text{ grams } Ni(Cr_{0.8}Fe_{0.2})_2O_4}{(5.229 \text{ g/cc})_{spinel}(0.35) + (2.10 \text{ g/cc})_{glass}(0.65)}$ = 1.70 x 10^5 cc slag could accumulate on the melter floor.
9	The surface area of the bottom of the DWPF melter is ~28 ft^2 or 2.6x10^4 cm^2
10	Dividing the volume of slag (spinel plus glass) from Step #8 by the area of the bottom of the melter (Step #9) provides the approximate depth of the slag deposits in centimeters: = (1.70 x 10^5 cc slag deposits)/(2.6x10^4 cm^2) = 6.55 cm slag in 1.75 years of operation with oxidizing feeds.
11	If a room temperature glass density of 2.75 g/cc is used for DWPF glass instead of the 2.10 g/cc at the melt temperature (see Step #8) then the slag deposit depth is calculated to be 5.82 cm slag in 1.75 years of operation with oxidizing feeds.

Table 1. Comparison of the Rate of Accumulation of Melter Bottom Deposits in the DWPF and in Large Scale Pilot Scale Melters that were Slurry Fed

Melter	Melt Pool Surface Area (m^2)	Measured Depth of Bottom Deposits (cm)	Continuous Operation (Years)	Amount of Glass Poured /Flowsheet	Calculated Slag Accumulation in Years operated (cm)
LSFM	1.12	0.17-1.27 [38]	2	240 tons/ reducing formic acid flowsheet	2.79
SGM	1.12	None [36, 47]	2	90 tons/ reducing formic acid flowsheet	No accumulation defined
IDMS	0.29	Indeterminate (30.5 cm) combined frozen cold cap and bottom deposits [39])	7	28 tons/ reducing formic acid flowsheet 8 tons / oxidizing nitric acid flowsheets	15.11
DWPF Melter #1 Non-Radioactive	2.6	~6.35 [42]	1.75	~105 tons* (oxidizing nitric acid flowsheet)	6.55
DWPF Melter #1 Radioactive	2.6	Unknown	7.25	~2713.5 tons (~2/3 oxidizing flowsheet and remainder reducing flowsheet)	27.10
DWPF Melter #2 Radioactive	2.6		~11	~4586.5 tons (reducing flowsheet)	41.12

* tons of glass poured by March 30, 1996 when the DWPF Melter #1 bottom was probed

Table 2. Relative Corrosion Rates of DWPF, Pilot Scale Melters, and Crucible Studies Using ASTM 621.

Scenario	Time Melter Operated or Assumed Operation (Years)	Average "loss of material" (mils/day)		Calculated Accumulation of Spinel-glass depth years of Operation (cm)	
Crucibles with oxidized feed [2]	1.75	1.57 from Equation 2 in Part I		6.55	
Part I (1/100th scale DWPF-Melt) [2]	1.75	2.29	1.41 average	11.15	6.85 average
Part I (1/100th scale DWPF-Vapor) [2]	1.75	0.52		2.54	
DWPF Design Basis (sidewall, lid, bottom) [48]	1.75	3.00		14.63	
DWPF Design Basis (melt line) from SCM Campaign 2 Maximum Wear 2-3 inches below melt line [48]	1.75	7.50		36.6	
DWPF Design Basis (wall below melt line) from SCM Campaign 2 Walls below melt line [48]	1.75	5.40		26.37	
LSFM overall [38]	2	0.50		2.79	
LSFM melt line [38]	2	1.00		5.58	
IDMS drain area – 7 years [39]	7	0.78		15.22	
Crucible SRNL165 glass [2]	1.75	0.68-0.79		3.61	
Crucible SRNL131 glass [2]	1.75	0.64		3.12	

* Assuming 35% spinel in 65% glass slag and all Cr_2O_3 from K-3 based on "average loss of material" per year of operation

Table 3. Chemical Composition of Glass and Crystalline Deposits Probed from the Bottom of the DWPF Melt Pool on March 30, 1996

OXIDE	MELTER FEED TANK (MFT) COMPOSITION RANGE (wt%)	DWPF CUP#1A GLASS OFF ROD (wt%)	DWPF CUP#1B GLASS OFF ROD (wt%)	DWPF CUP#2A GLASS IN CUP (wt%)	DWPF CUP#2B GLASS IN CUP (wt%)	DWPF CUP #1A BOTTOM (wt%)	DWPF CUP#1B BOTTOM (wt%)	DWPF CUP#2A BOTTOM (wt%)	DWPF CUP#2B BOTTOM (wt%)
	MFT #17 + 18	**Melt Pool Glass in Sampler Cups and Adhering to 304L Rod**				**Melter Bottom Deposits Adhering to Bottom of Sampler Cups**			
		ADS #30070545	**ADS #30070546**	**ADS #30070549**	**ADS #30070550**	**ADS #30070543**	**ADS #30070544**	**ADS #30070547**	**ADS #30070548**
Al_2O_3	4.89-4.63	4.74	4.77	4.60	4.65	4.34	4.36	4.28	4.13
B_2O_3	7.69-9.53	7.88	7.75	7.51	7.27	6.89	6.85	6.11	6.63
BaO	---	0.06	0.06	0.05	0.05	0.05	0.05	0.05	0.06
CaO	0.98-1.07	0.89	0.97	0.97	0.85	0.81	0.82	0.77	0.78
Cr_2O_3	**0.13-0.12**	**0.45**	**0.45**	**0.52**	**0.50**	**1.21**	**1.16**	**1.42**	**1.61**
Cu_2O	---	0.16	0.16	0.15	0.15	0.16	0.16	0.15	0.15
CuO	0.39-0.37	0.17	0.17	0.16	0.16	0.18	0.18	0.17	0.17
Fe_2O_3	**10.44-11.37**	**11.29**	**11.12**	**12.09**	**11.72**	**16.05**	**15.70**	**14.77**	**16.51**
K_2O	2.31-1.72	1.94	1.98	1.89	1.92	1.79	1.76	1.74	1.71
Li_2O	3.92-3.95	3.80	3.74	3.65	3.49	3.42	3.39	3.23	3.32
MgO	1.73-1.90	1.64	1.62	1.59	1.54	1.54	1.53	1.40	1.50
MnO	2.12-1.88	1.98	1.95	2.03	1.97	2.43	2.40	2.13	2.37
Na_2O	10.31-11.77	10.70	10.78	10.32	10.46	9.59	9.58	9.31	9.02
NiO	**0.7-0.47**	**0.73**	**0.71**	**1.40**	**1.37**	**3.46**	**3.36**	**3.25**	**3.68**
P_2O_5	---	0.12	0.10	0.09	0.11	0.10	0.12	0.08	0.08
PbO	---	---	---	---	---	---	0.06	---	0.13
SiO_2	48.3-53.54	50.05	49.24	47.89	47.33	44.36	43.66	38.08	42.31
SrO	---	0.05	0.05	0.05	0.05	0.05	0.05	0.04	0.05
TiO_2	0.30-0.23	0.28	0.28	0.27	0.27	0.27	0.27	0.28	0.26
ZnO	---	0.06	0.06	0.07	0.07	0.09	0.08	0.15	0.08
ZrO_2	0.80-0.59	0.74	0.76	0.72	0.73	0.74	0.75	0.70	0.67
SUMS	95.01-103.11	97.70	96.70	96.02	94.63	97.51*	96.28*	88.09**	95.20*
$Fe^{+2}/\sum Fe$	BDL	BDL	BDL	BDL	BDL	0.04	0.04	0.04	0.04

* Note from analyst that the entire sample did not dissolve

** Note from analyst that sample did not flux/did not completely dissolve

Table 4 Quantitative Phase Analysis of Glass and Crystalline Deposits Probed from the Bottom of the DWPF Melt Pool on March 30, 1996

Sample ID	Wt% Spinel by XRD	Wt% RuO_2 by XRD
Glass in Sample Cups	None detected	None detected
Side of Rod (primarily glassy)	0.7	None detected
Bottom of Rod -small sample	None detected	0.9
Bottom of Rod -large sample	5.2	0.3
Cup bottom-A	25	None detected
Cup bottom-B	34	None detected

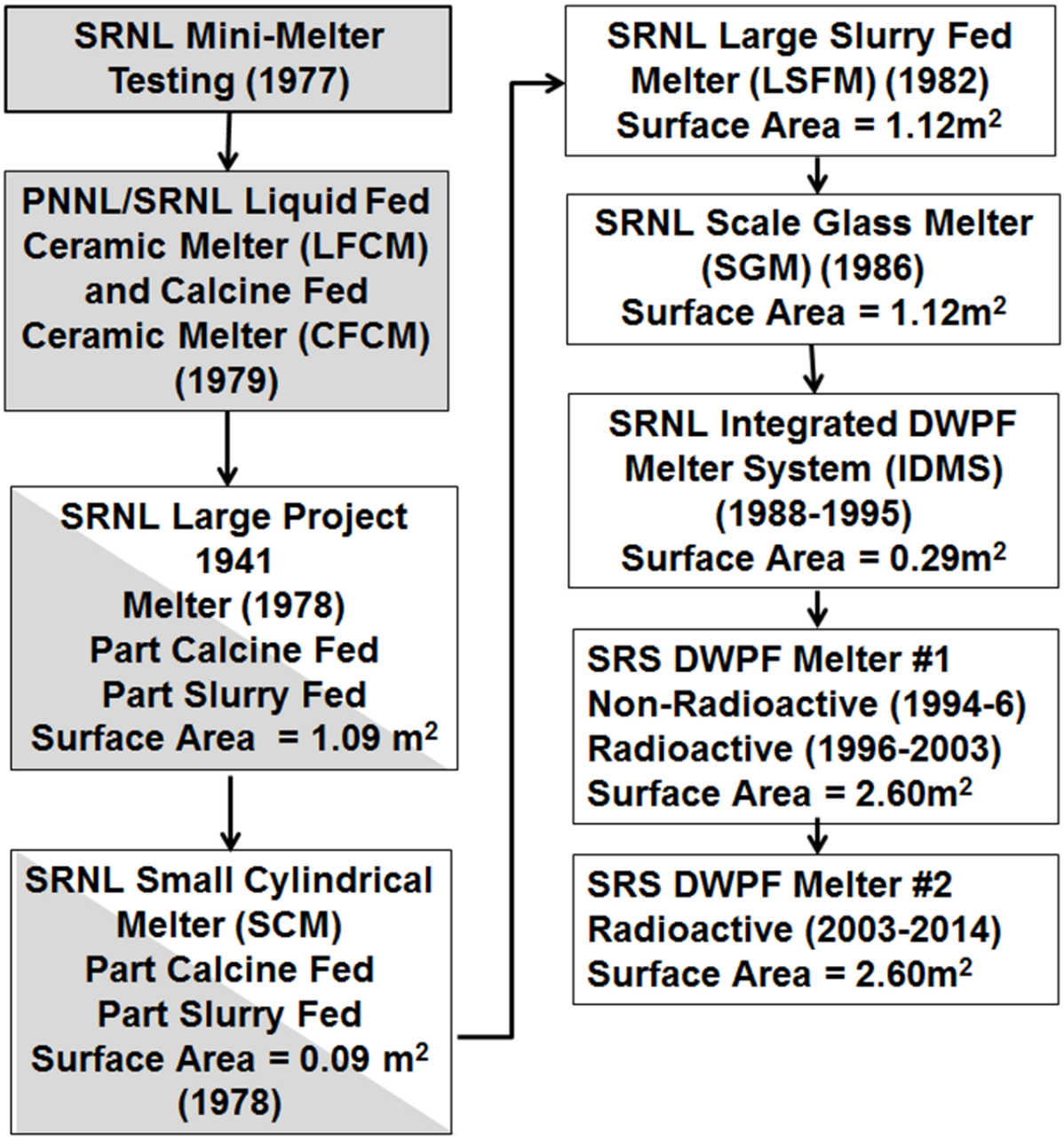

Figure 1. Timeline of pilot-scale melters used to determine DWPF design parameters including K-3 corrosion rates. Note that the shaded boxes are for melters that were calcine fed all or part of the time and the remaining melters were slurry fed. Slurry feeding is the DWPF reference methodology. The relative melt pool surface area for each melter is given in m^2.

REFERENCES

1 Certa, P.J. and M.N. Wells, **"River Protection Project System Plan,"** ORP-11242, Rev. 5, DOE Office of River Protection, Richland, WA (November 2010).

2 C.M. Jantzen, K.J. Imrich, K.G.Brown, and J.B. Pickett, **"High Chrome Refractory Characterization: Part I. Impact of Melt Pool REDuction/Oxidation (REDOX) on the Corrosion Mechanism in Radioactive Waste Glass Melters,"** this journal.

3 H.N. Guerrero and D.F. Bickford, **"DWPF Melter Air-Lift Bubbler: Development and Testing for Increasing Glass Melt Rates and Waste Dissolution,"** U.S. DOE Report WSRC-TR-00196, Rev. 0 (May 2002). Also US Patent #7,225,643 (June 5, 2007).

4 M.E. Smith and D.C. Iverson, **"Installation of Bubblers in the Savannah River Site Defense Waste Processing Facility Melter,"** U.S. DOE Report SRR-STI-2010-00784 and WM11 Paper # (2010-2011).

5 C.M. Jantzen, **"Relationship of Glass Composition to Glass Viscosity, Resistivity, Liquidus Temperature, and Durability: First Principles Process-Product Models for Vitrification of Nuclear Waste,"** Ceramic Transactions, 23, American Ceramic Society, Westerville, OH, 37-51 (1991).

6 C.M. Jantzen, D.F. Bickford, and D.G. Karraker, **"Time-Temperature Transformation Kinetics in SRL Waste Glass,"** Advances in Ceramics, 8, American Ceramic Society, Westerville, OH, 30-38 (1984).

7 D.F. Bickford and C.M. Jantzen, **"Devitrification of SRL Defense Waste Glass**," Scientific Basis for Nuclear Waste Management, VII, G.L. McVay (Ed.), Elsevier Publ, New York, 557-565 (1984).

8 C.M. Jantzen and D.F. Bickford, **"Leaching of Devitrified Glass Containing Simulated SRP Nuclear Waste,"** Scientific Basis for Nuclear Waste Managment, VIII, C.M.Jantzen, J.A. Stone, and R.C. Ewing (Eds.), Materials Research Society, Pittsburgh, PA, 135-146 (1985).

9 D.F. Bickford and C.M. Jantzen, **"Devitrification of Defense Nuclear Waste Glasses: Role of Melt Insolubles,"** J. Non-Crystalline Solids, 84, 299-307 (1984).

10 S.L. Marra, M.K. Andrews, and C.A. Cicero, **"Time-Temperature-Transformation Diagrams for DWPF Projected Glass Compositions,"** Proceedings of the Environmental and Waste Management Issues in the Ceramic Industry, G.B. Mellinger (Ed.), Ceramic Transactions, V. 39, Am. Ceram. Soc., Westerville, OH, 283-302 (1994).

11 C.M. Jantzen and K.G. Brown, **"Predicting the Spinel-Nepheline Liquidus for Application to Nuclear Waste Glass Processing: Part I. Primary Phase Analysis, Liquidus Measurement, and Quasicrystalline Approach,"** J. Am. Ceramic Soc., 90 [6], 1866-1879 (2007).

12 C.M. Jantzen and K.G. Brown, **"Predicting the Spinel-Nepheline Liquidus for Application to Nuclear Waste Glass Processing: Part II. Quasicrystalline Freezing Point Depression Model,"** J. Am. Ceramic Soc. 90 [6], 1880-1891 (2007).

13 C.M. Jantzen, D.F. Bickford, and D.G. Karraker, **"Time-Temperature-Transformation Kinetics in SRL Waste Glass,"** Advances in Ceramics, 8, American Ceramic Society, Westerville, OH, 30-38 (1984).

14 C.M. Jantzen, **"Devitrification of Scale Melter Glass in Riser Heater,"** U.S. DOE Report DPST-86-461 (1986).

15 P.A. Bingham, A.J. Connelly, N.C. Hyatt, and R.J. Hand, **"Corrosion of Glass Contact Refractories for the Vitrification of Radioactive Wastes: A Review",** Intl Materials Reviews 56 [4] 226 (2011).

16 S. Zhang and W.E. Lee, **"Use of Phase Diagrams in Studies of Refractories Corrosion,"** Intl. Materials Reviews. 45 [2] 41-58 (2000).

17 W.E. Lee and S. Zhang, **"Melt Corrosion of Oxide and Oxide-Carbon Refractories,"** Intl. Materials Reviews, 44[3], 77-104 (1999).

18 W.E. Lee and R.E. Moore, **"The Evolution of *in situ* Refractories in the 20th Century,"** J. Am. Ceram. Soc. 81 [6] 1385-1410 (1998).

19 W.E. Lee, S. Zhang, and H. Sarpoolaky, **"Different Types of *in situ* Refractories,"** Ceramic Transactions 125, American Ceramic Society, pp.245-252 (2001).

20 W.N. Rankin, P.E. O'Rourke, P.D. Soper, M.B. Cosper, and B.C. Osgood, **"Evaluation of Corrosion and Deposition in the 1941 Melter,"** U.S. DOE Report DPST-82-231, E.I. duPont deNemours & Co., Savannah River Laboratory, Aiken, SC (March, 1982).

21 S.A. Cooper and P.S. Nicholson, **"Influence of Glass Redox Conditions on the Corrosion of Fusion-Cast Chrome-Alumina Refractories,"** Ceramic Bulletin, 59[7], 715-717 (1980).

22 M.J. Plodinec, **"Rheology of Glasses Containing Crystalline Material,"** Advances in Ceramics, V. 20, Nuclear Waste Management II, D.E. Clark, W.B. White, and A.J. Machiels (Eds.), Am. Ceram. Soc., Westerville, OH, 117-124 (1986).

23 M.J. LaMont and P. Hrma, **"A Crucible Study of Spinel Settling in a AHigh-Level Waste Glass,"** Ceramic Trans. V. 87, 343-348 (1998).

24 J. Klouzek, J. Alton, P. Hrma, and T. Plaisted, **"Crucible Study of Spinel Settling in Molten High-Level Waste Glass,"** Ceramic Trans. V. 119, 301-308 (2001)

25 Battelle Memorial Institute, **"Engineering Properties of Selected Ceramic Materials,"** American Ceramic Society, Columbus, OH, p.5.5.5-1 (1966).

26 C.M. Jantzen, K.G. Brown, K.J. Imrich, and J.B. Pickett, **"High Cr_2O_3 Refractory Corrosion in Oxidizing Melter Feeds: Relevance to Nuclear and Hazardous Waste**

Vitrification Ceramic Transactions, v. 93, J.C. Marra and G.T. Chandler (Eds.), American Ceramic Society, Westerville, OH, 203-212 (1999).

27 M.J. Plodinec, **"Long-Term Waste Management Progress Report Small-Scale Electric Meter, II. Slag Formation,"** U.S. DOE Report DPST-78-453, E.I. duPont deNemours & Co., Savannah River Laboratory, Aiken, SC (August, 1978).

28 M.J. Plodinec, **"Long-Term Waste Management Progress Report Small-Scale Electric Meter, IV. Effects of Feed Mixing and Segregation on Glass Melting,"** U.S. DOE Report DPST-79-227, E.I. duPont deNemours & Co., Savannah River Laboratory, Aiken, SC (January, 1979).

29 J.P. Moseley and M.B. Cosper, **"An Analysis of Spinel Deposition in the 1941 Melter,"** U.S. DOE Report DPST-81-587, E.I. duPont deNemours & Co., Savannah River Laboratory, Aiken, SC (July, 1981).

30 G.G. Wicks and W.N. Rankin, **"Microstructural Analysis of Slag Formation in Battelle's Calcine Fed Ceramic Melter (CFCM),"** U.S. DOE Report DPST-79-372, E.I. duPont deNemours & Co., Savannah River Laboratory, Aiken, SC (April, 1979).

31 K.R. Routt, M.J. Plodinec, and M.A. Porter, **"Performance of Structural and Active Components of the Small Cylindrical Melter: Second Operating Campaign,"** U.S. DOE Report DPST-80-654, E. I. duPont deNemours &Co., Aiken, SC (December 1, 1980).

32 W.N. Rankin, P.E. O'Rourke, P.D. Soper, M.B. Cosper, and B.C. Osgood, **"Evaluation of Corrosion and Deposition in the 1941 Melter,"** U.S. DOE Report DPST-82-231, E.I. duPont deNemours & Co., Savannah River Laboratory, Aiken, SC (March, 1982).

33 R.D. Dierks**, "The Design and Performance of a 100-kg/hr, Direct Calcine-Fed Electric Melter System for Nuclear Waste Vitrification,"** U.S. DOE Report PNL-3387, Richland, WA (1980).

34 S.M. Barnes and D.E. Larson, **"Materials and Design Experience in a Slurry-Fed Electric Glass Melter,"** U.S. DOE Report PNL-3959, Richland, WA (1981).

35 C.M. Jantzen, A.D. Cozzi, and N.E. Bibler, **"Characterization of Defense Waste Processing Facility (DWPF) Glass and Deposit Samples from Melter #2,"** U.S. DOE Report WSRC-TR-2003-00504 (March 2004).

36 C.M. Jantzen, **"Lack of Slag Formation in the Scale Glass Melter,"** U.S. DOE Report DPST-87-373, E.I. duPont deNemours & Co., Savannah River Laboratory, Aiken, SC (April, 1987).

37 S.R. Young and D.F. Bickford, **"A Review of DWPF Pilot Melter Experience - Melt Rate and Associated Parameters,"** U.S. DOE Report WSRC-TR-96-0405, Westinghouse Savannah River Co., Savanannah River Technology Center, Aiken, SC (December, 1996).

38 D.C. Iverson and D.F. Bickford, **"Evaluation of Materials Performance in a Large-Scale Glass Melter After Two Years of Vitrifying Simulated SRP Defense Waste,"** Sci. Basis for Nucl. Waste Mgt., VIII, Mat. Res. Soc., Pittsburgh, PA, 839-845 (1985).

39 C.M. Jantzen and D.P. Lambert, **"Inspection and Analysis of the Integrated DWPF Melter System (IDMS) After Seven Years of Operation,"** U.S. DOE Report WSRC-RP-575, Westinghouse Savannah River Co., Aiken, SC (February, 1997).

40 A. Muan and E.F. Osborn, **"Phase Equilibria Among Oxides in Steelmaking,"** Addison-Wesley Publishing Company, Inc., Reading, MA, 236pp. (1965).

41 G.L. Smith, D.K. Peeler, H.D. Smith, P .A. Smith, E.M. Tracey, and K.D. Wiemers, **"Effect of Feed Chemistry on Waste Melter Vitrification Kinetics,"** U.S. DOE Report, PVTD-T3C-95-129, Pacific Northwest Laboratory, Richland, WA (September, 1995).

42 R.T. Jones, **"DWPF Melter Pour Stream Anomaly-3/96 Investigation Compendium"**, Westinghouse Savannah River Company Memorandum HLW-APA-960027, Rev. 1, Westinghouse Savannah River Company, Aiken, SC (May 2, 1996).

43 C. Allaire, **"Interfacial Phenomena,"** Ceramic Transactions 125, American Ceramic Society, 289-307 (2001).

44 C. Allaire, **"Mechanism of Corundum Growth in Refractories Exposed to Al-Mg Alloys,"** Aluminum Transactions, 3[1] 105-120 (2000).

45 W.N. Rankin, **"Corrosion of Melter Materials, III: Effect of Na2O,"** U.S. DOE Report DPST-81-933 (February 1982).

46 **"Preliminary Technical Data Summary for the Defense Waste Processing Facility, Stage 1,"** U.S. DOE Report DPSTD-80-38, E.I. duPont deNemours & Co., Savannah River Plant, Aiken, SC (September, 1980).

47 M.R. Baron and M.E. Smith, **"Summary of the Drain and Restart of the DWPF Scale Glass Melter, "** U.S. DOE Report DPST-88-481, E.I. duPont deNemours & Co., Savannah River Laboratory, Aiken, SC (May, 1988).

48 "**Basic Data Report Defense Waste Processing Facility Sludge Plant Savannah River Site 200-S Area,"** U.S. DOE Report, WSRC-RP-92-1186 (DPSP 80-1033), Westinghouse Savannah River Company, Aiken, SC, Part 20, Items 230, Rev. 139, (July, 1992).